Electrochemical characteristics of titanium based biomaterials in artificial saliva

D. Mareci*, G. Ungureanu, D. M. Aelenei and J. C. Mirza Rosca

In the last decade, new titanium alloys have been developed in different areas of dentistry, such as Ti6Al7Nb, Ti6Al2Nb1Ta1Nb, and Ti5Al2.5Fe. The aim of this study was to compare the Ti6Al7Nb, Ti6Al2Nb1Ta1Nb, Ti5Al2.5Fe, and Ti6Al4V alloys with the commercial titanium, regarding the corrosion resistance in artificial saliva. In the electrochemical estimations the polarization data are converted into instantaneous corrosion rate values (I_{corr}). The passivation properties were comparable for the four alloys. The EIS spectra are best fitted using an equivalent circuit (EC), which corresponds to the model of a two-layer structure for the passive film. High impedance values (in the order of $10^6\ \Omega\ cm^2$) were obtained from medium to low frequencies for all materials suggesting high corrosion resistance in artificial saliva.

The electrochemical and corrosion behavior of Ti6Al4V is not affected on substituting vanadium with niobium, iron, molybdenum, and tantalum.

1 Introduction

The corrosion process is one of the essential phenomenon that determines the biocompatibility of dental alloys.

Commercial titanium and titanium alloys are used on a large scale in restorative dentistry due to their advantages as compared with other similar materials: chemical inertia [1], low densities [2], toxicity absence [3], and increased biocompatibility [4]. Corrosion resistance is determined by the formation of an adherent titanium oxide layer, of reduced thickness, on titanium or titanium alloys surface. This film contains as a major compound TiO_2 with anionic gaps, which confer the n semiconductor character [5]. This film functions as a barrier *versus* the metal tendency to interact with the corrosion medium. The film formation is enhanced by alloying with transitional metals having d unsaturated orbitals, when solid solutions with Cu, Mo, W, Nb or inter-metallic compounds with Pt, Ni may appear. The increase in the oxide film thickness conducts to the formation of both a crystalline layer and another porous layer. The last layer contains hydrated oxides with 30% water content.

The titanium is difficult to cast because it has a high melting point value (1682 °C) and presents the tendency of contamination due to an increased reactivity.

In order to decrease the quantity of melting impurities and to increase the wear resistance the titanium is alloyed with various elements. The titanium alloys having a biphasic structure ($\alpha + \beta$) are used on a large scale. Among the alloying elements, Al is α-stabilizer and it dissolves in the α-phase increasing the stability domain of this phase. Mo, V, Nb, and Ta are β-stabilizer elements which decrease the temperature of allotropic transformation, forming continuous series of solid solutions with β-Ti but their solubility in α-Ti is limited. Fe is an element β-stabilizer forming with the titanium eutectic and eutectoids phases.

Corrosion of metal implants is critical because it can adversely affect the biocompatibility and mechanical integrity. The material used must not cause any biological reaction in the body and it must be stable and retain its functional properties. Corrosion and surface film dissolution are two mechanisms for introducing additional ions in the body.

Extensive release of metal ions from prosthesis can result in adverse biological reactions and lead to mechanical failure of the device.

The ''standard'' Ti6Al4V was one of the first titanium biomaterials introduced in implantable components and devices (particularly for applications in orthopedics and osteosynthesis). Although this alloy is still widely used in medicine, some concerns have been recently expressed over its use since it appears that small amounts of vanadium, released in the human body, induce possible cytotoxic effect. Thus, the toxicity of alloying elements like V of conventional Ti6Al4V alloy has required the development of new titanium alloys with non-toxic elements (Nb, Zr, Ta, Mo, Fe, etc.).

The modification of dental alloys' properties could be determined using rapid electrochemical tests considered as a qualitative criterion to estimate its corrosion resistance.

The electrochemical techniques most commonly used for corrosion studies have their own specific advantages for addressing effectively certain aspects of the electrochemical performance of implant materials [6]. The direct current (DC) polarization curves can show the potential region in which the passivity is effectively maintained and the alternative current (AC) impedance method, being a non-destructive electrochemical technique, is particularly useful for monitoring certain electrochemical changes as a function of time.

* *D. Mareci, G. Ungureanu, D. M. Aelenei*
Faculty of Chemical Engineering, Technical University ''Gh. Asachi'' Iasi,
B-dul D. Mangeron, no. 71A, 700050 Iasi (Romania)
E-mail: danmareci@yahoo.com

J. C. Mirza Rosca
Las Palmas de Gran Canaria University,
35017 Las Palmas de Gran Canaria (Spain)

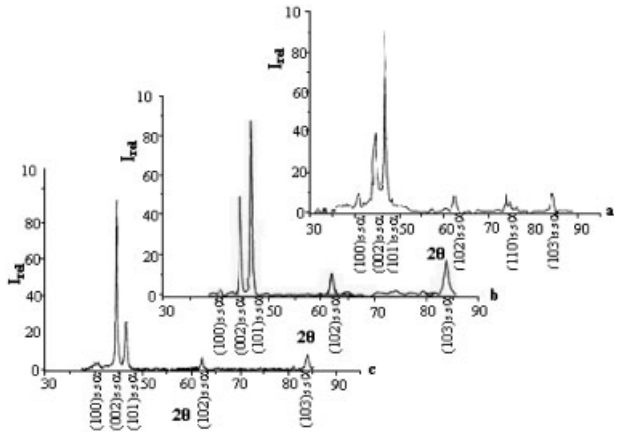

Fig. 1. X-ray patterns: (a) Ti6Al7Nb alloy, (b) commercial titanium, and (c) Ti5Al2.5Fe alloy

Therefore, the combination of these techniques is often necessary to obtain the most comprehensive information about the corrosion behavior under given circumstances.

DC electrochemical methods are commonly used to evaluate corrosion, but over the past decade many articles on the electrochemical impedance spectroscopy (EIS) have been published [7–17]. *Kovacs* [18] has demonstrated that the AC impedance method is particularly useful when some electrochemical behavior changes as a function of time are recorded, because it is a non-destructive technique.

This paper analyses the electrochemical corrosion behavior and the characterization of passive film formed on various titanium alloys in artificial saliva comparatively with a commercial titanium sample.

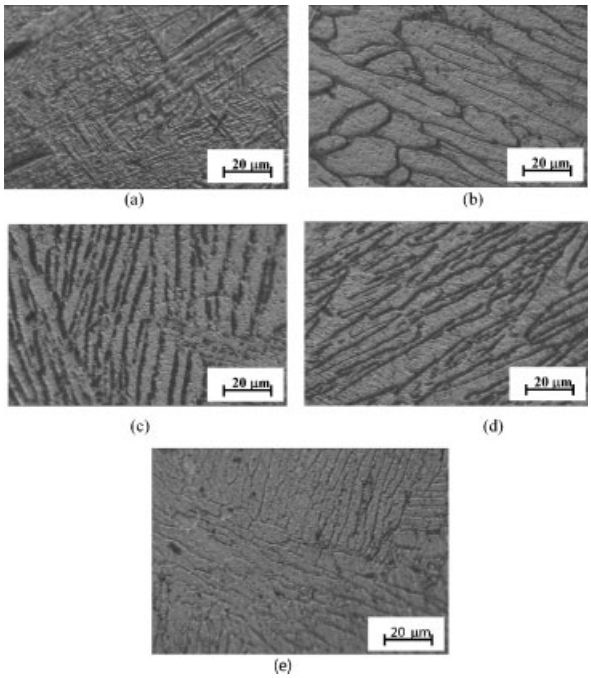

Fig. 2. Micrographs for: (a) commercial titanium, (b) Ti6Al7Nb alloy, (c) Ti6Al2Nb1Ta1Nb, (d) Ti6Al4V, and (e) Ti5Al2.5Fe

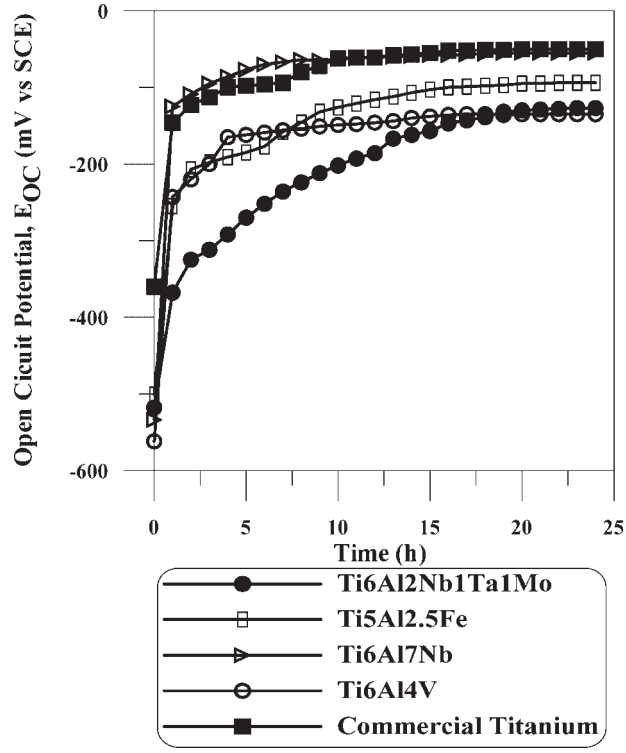

Fig. 3. Open circuit potential (E_{OC}) *versus* time in artificial saliva for commercial titanium and titanium alloys

2 Materials and methods

Titanium alloys were purchased from the Rare and Non-Ferrous Metals Institute, Bucharest, as cast having a rod like shape. The titanium-based materials in this work used were: commercial titanium (99.99% Ti), Ti6Al4V, Ti6Al2Nb1Ta1Mo, Ti6Al7Nb, and Ti5Al2.5Fe alloys.

The structural studies were performed with an optical microscope (Olympus PME 3-ADL) and the qualitative phase analysis by X-ray diffraction (DRON 2 X-ray diffractometer; Co Kα radiation, 20 kV).

The microstructures were revealed by etching in 10% HF + 5% HNO_3 solution for 3–5 s at 25 °C.

As corrosion medium was used a solution of aerated artificial saliva Carter-Brugirard AFNOR/NF (French Association of Normalization). Saliva composition was: NaCl, 0.7 g/L; KCl, 1.2 g/L; $Na_2HPO_4H_2O$, 0.26 g/L; $NaHCO_3$, 1.5 g/L; KSCN, 0.33 g/L; and carbamide, 1.35 g/L [19].

The pH was measured with a multiparameter analyzer CONSORT 831C. The pH of this reference saliva was 8.

Table 1. Open circuit potential values (initial and after 24 h of alloys samples' immersion in artificial saliva)

Material	Open circuit potential, E_{OC} (mV *vs.* SCE)	
	Initial	After 24 h of immersion
Ti5Al2.5Fe	−501	−94
Ti6Al2Nb1Ta1Mo	−518	−127
Ti6Al7Nb	−534	−55
Ti6Al4V	−562	−135
Commercial Titanium	−360	−50

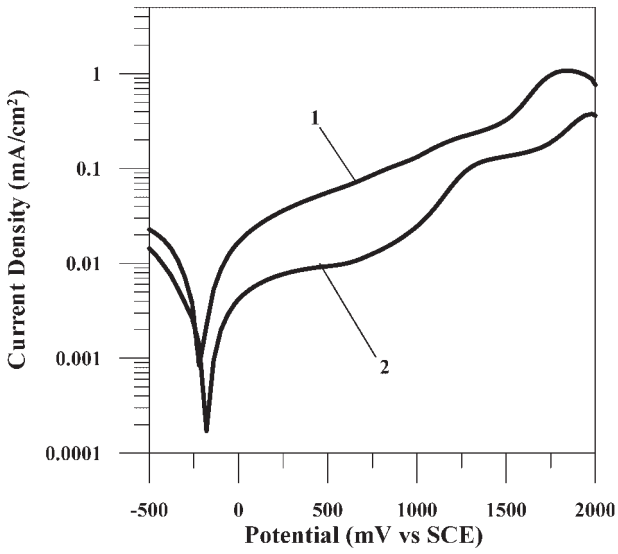

Fig. 4. The potentiodynamic polarization curves for the Ti5Al2.5Fe alloy (1, after 24 h of immersion in artificial saliva; 2, after 7 days of immersion in artificial saliva)

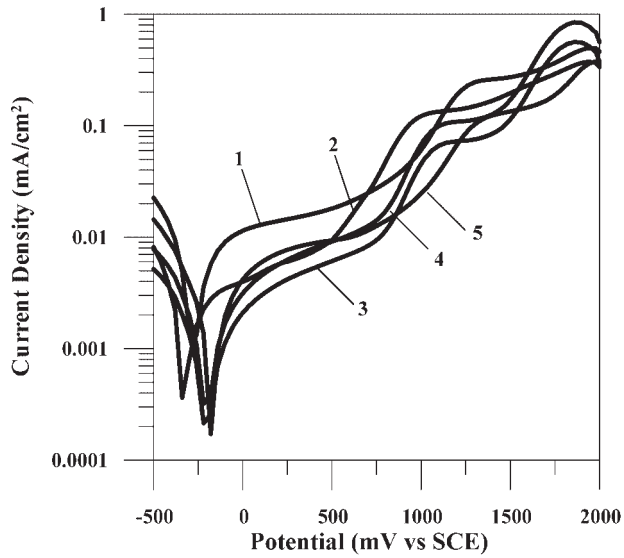

Fig. 5. The potentiodynamic polarization curves for the: 1, Ti6Al2Nb1Ta1Mo alloy; 2, commercial titanium; 3, Ti6Al7Nb alloy; 4, Ti6Al4V alloy; and 5, Ti5Al2.5Fe alloy (after 7 days of immersion in artificial saliva)

Electrochemical measurements were carried out at 25 °C and began after 7 days of immersion in artificial saliva in order that the passive film may be formed as a result of electrochemical reactions with the artificial saliva.

All the electrochemical measurements were performed with a PAR 263 A potentiostat connected with a PAR 5210 lock-in amplifier. A saturated calomel electrode (SCE) was used as a reference and platinum as an auxiliary electrode. Experimental data were acquired and processed with the PowerCorr and ZSimWin software.

The working electrodes, processed in cylindrical shape and mounted in a tetrafluoroethylene support, present a one-dimensional circular area, which is exposed to corrosion and measured.

Before the experimental tests the samples were mechanically polished with SiC abrasive paper up to a granulation number of 2,500, then polished using 1 μm alumina suspension, degreased in ethanol, and rinsed with distilled water.

The electrochemical techniques used for the corrosion behavior study were: potential measurements, polarization curves, and EIS. The tests were normally repeated two or three times, to ensure that they presented reasonable reproducibility.

The corrosion process was characterized by several electrochemical quantities:

– The open circuit potential (E_{OC}), recorded for 24 h with the sample immersed in an aerated electrolyte.
– The polarization resistance (R_p), calculated from traces of the polarization curve at ±10 mV *versus* E_{OC}. The scanning rate was 0.166 mV/s.
– The Tafel slopes (b_a and b_c) and the corrosion current (I_{corr}) using the *Stern–Geary* [20] equation:

$$I_{corr} = \frac{b_a b_c}{2,3R_p(b_a + b_c)} \quad (1)$$

The Tafel slopes were calculated from plots of the polarization curves at ±150 mV *versus* E_{OC}. The scanning rate was 0.5 mV/s.
– Potentiodynamic polarization curves were obtained with a scan rate of 10 mV/s in the potential range –500 mV to +2000 mV/SCE.
– EIS measurements were carried out at E_{OC} and at 400 mV/SCE in aerated solutions. The spectra were recorded in the 10^{-2}–10^5 Hz frequency range. The applied alternating potential signal had the amplitude of 10 mV.

3 Analysis of impedance spectra

For the analysis of the impedance data, a software program ''ZSimWin'' was used. The program used a variety of electrical circuits to numerically fit the measured impedance data. The program is capable of conducting analysis of

Table 2. The main parameters of corrosion process after 7 days of immersion in artificial saliva

Material	E_{corr} (mV)	R_p (Ω cm^2)	b_a (mV/dec)	b_c (mV/dec)	I_{corr} (nA/cm^2)	I_{pass} (μA/cm^2)	E_{tr} (mV/SCE)
Commercial Titanium	−260	1.5×10^6	171	125	21	9.5	710
Ti6Al4V	−230	9.3×10^5	159	115	31	10	810
Ti6Al7Nb	−220	9.6×10^5	164	121	32	9	860
Ti5Al2.5Fe	−180	1×10^6	170	118	30	6	880
Ti6Al2Nb1Ta1Mo	−340	9×10^5	155	105	30	17	800

E_{corr}, corrosion potential; R_p, polarization resistance; b_c and b_a, Tafel slopes; I_{corr}, density of corrosion current; I_{pass}, passive current densities; and E_{tr}, transpassivation potential.

heavily convoluted frequency dispersion data by deconvoluting the complex response into those of simple subcomponents. This approach combined with the general nonlinear least squares fit procedure allowed us to construct an equivalent circuit (EC), whose simulated responses fit actually measured data well. After each experiment, the AC impedance data were displayed as Bode plots (Zmod *vs.* frequency, and phase angle *vs.* frequency, where Zmod is the absolute value of the impedance). The advantage of the Bode plot is that the data for all measured frequencies are shown and that a wide range of impedance values can be displayed. The frequency dependence of the phase angle indicates whether one or more time constants occur and can be used to determine the values of the parameters in the EC.

4 Results and discussion

For all the investigated titanium-based materials, the qualitative phase analysis by X-ray diffraction shows that the main phase is the α solid solution. Figure 1 shows the X-ray patterns for the Ti6Al7Nb, Ti5Al2.5Fe alloys, and commercial titanium.

As-cast titanium-based materials have a structure that is determined by the cooling from β-phase domain, and a moderate cooling rate. The commercial titanium has a monophasic structure that contains polycrystalline α-phase (hexagonal close packed). The α-phase has a feather-like morphology (Fig. 2(a)). The investigated titanium alloys have a Widmanstätten-type structure that consists of α-phase lamellae. The optical images from Figs. 2(b–e) show a basket weave morphology of α-phase regardless of chemical compositions of titanium alloys.

Metals immersed in an electrolytic environment generate an electric potential that varies with time. It stabilizes to a stationary value after a period of immersion. As is the case for any surface phenomenon, this potential may vary with time because changes in the nature of the surface of the electrode occur (oxidation, formation of the passive layer or immunity). The alloys in the series with the most active (negative) potentials will generally tend to undergo more significant corrosion, while the other alloys (with positive potential values) will generally suffer less attack. The open circuit potential is used as a criterion for the corrosion behavior. This approach is qualitative and remains insufficient for a complete analysis.

Figure 3 shows the E_{OC} curves for all five stationary samples immersed in artificial saliva at 25 °C.

Following the immersion, an abrupt E_{OC} displacement towards positive potentials was noticed in Fig. 3 during a period of 1–2 h. Afterwards, the E_{OC} remained slowly increasing suggesting the growth of a film onto the metallic surface.

Solution treated specimens did not exhibit potential drops associated with surface activation during 24 h exposure in the artificial saliva. This kind of behavior strongly suggests that the air-formed native oxide consisting of TiO_2, Al_2O_3, and traces of Nb_2O_5, Fe_2O_3, Mo_2O_5, and Ta_2O_5 is thermodynamically resistant to chemical dissolution in artificial saliva. It was observed that the corrosion resistance of titanium alloys with Nb and Fe is marginally better than that of the Ti6Al4V alloy under physiological conditions (pH = 8). This was explained by the lower solubility of the Nb ion in comparison with Al and V in the Ti6Al4V [21].

In Table 1 open circuit potential values both at the initial moment and after 24 h of immersion in artificial saliva are presented.

Although after approximately 15–20 h the open circuit potential is stabilized, the passivation process continues as indicated by the two polarization curves (Fig. 4) registered for the Ti5Al2.5Fe alloy with the surface maintained 24 h and 7 days, respectively, in artificial saliva.

Thus, the change in corrosion potential with respect to time to more anodic values and the decrease of the passivation current were determined. From that reason the electrochemical tests were performed on materials with the surface maintained for 7 days in artificial saliva.

The polarization resistance (R_p) was determined by the tangent of the polarization curve (±10 mV *vs.* OCP) at I = 0. The R_p is representative for the degree of protection of the passivation layer of the alloy surface. The more the value of R_p increases, the more the alloys will resist against corrosion. For highly corrosion-resistant materials the R_p may even reach 10^6 Ω cm^2 [22].

The results of R_p are shown in Table 2. All samples are characterized by high values of the polarization resistance (10^6 Ω cm^2).

The Tafel slopes (b_a and b_c) were determined by fitting a theoretical polarization curve to the experimental polarization curve plotted in a range of ±150 mV *versus* E_{OC}. The corrosion current (I_{corr}) is representative of the degree of degradation of the alloy. An alloy with a tendency toward passivation will have a value of b_a greater than b_c, whereas an alloy that corrodes will have a b_a less than b_c [23].

Values of b_c amount to -115 ± 10 mV/decade (Tafel-like behavior). These values suggest that the hydrogen evolution reaction is independent of the alloying elements.

The high value of b_a in comparison with the values of b_c for all four alloys indicates an anodic control in the corrosion process. The control implies the existence of a passive layer on the material surface. The oxide layer on the alloys gives rise to a typical passive state with a low corrosion current density, as can be observed in Table 2. Corrosion current density has values of nanoampere order.

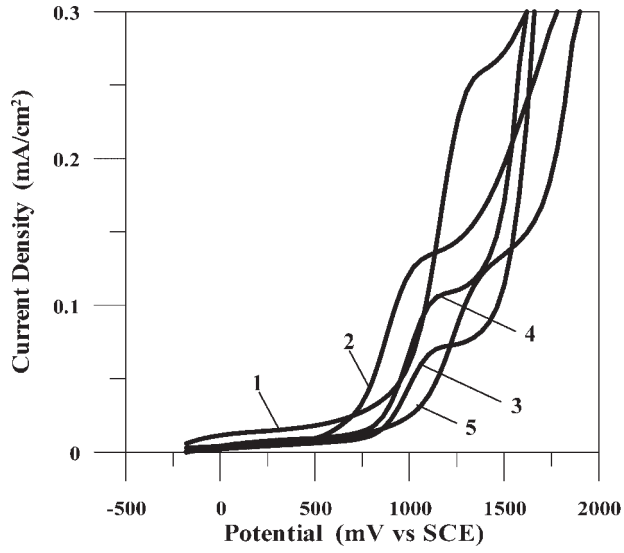

Fig. 6. Potentiodynamic polarization curves presented on linear axes in order to reveal the transpassivation potential for the: 1, Ti6Al2Nb1Ta1Mo alloy; 2, commercial titanium; 3, Ti6Al7Nb alloy; 4, Ti6Al4V alloy; and 5, Ti5Al2.5Fe alloy (after 7 days of immersion in artificial saliva)

Because the corrosion current densities (I_{corr}) of all the samples are comparable it is noted that the corrosion rates of the samples are comparable.

Similar polarization curves were obtained for all the samples after 7 days of immersion in artificial saliva (Fig. 5).

The nature of the potentiodynamic polarization curves indicated that all the samples are passivating immediately at immersion in the artificial saliva; all five materials translated directly from the ''Tafel region'' into a stable passive state, without exhibiting a common active–passive transition. The polarization behavior can be termed as stable passivity. This behavior was noted for all the samples.

The corrosion potentials (E_{corr}) determined from the polarization curves are lower than those obtained from the open circuit potential measurements. This is expected, because the polarization tests were started at a cathodic potential relatively to the corrosion potential, so that the passive film at the surface at least partially was removed due to the highly reducing initial potentials.

Figure 6 shows, in linear representation, the part of the polarization curves for all the five samples, in the scale of anodic currents between 0 and 300 $\mu A/cm^2$. This helps to visualize the transpassivation potential, another electrochemical quantity that characterizes the corrosion behavior

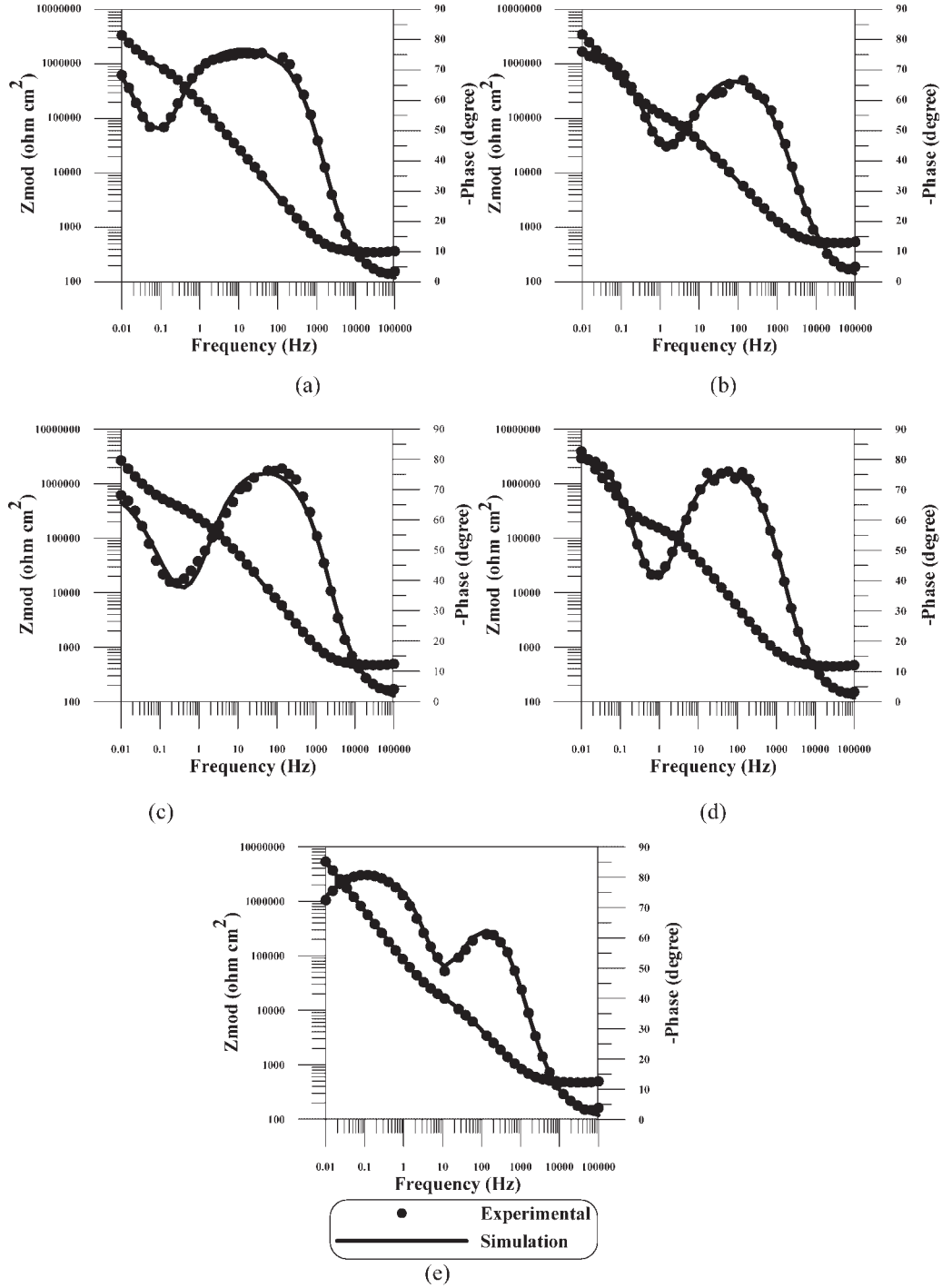

Fig. 7. Bode plots of tested materials recorded at open circuit potential after immersion for 7 days in artificial saliva: (a) Ti6Al2Nb1Ta1Mo alloy, (b) commercial titanium, (c) Ti6Al7Nb alloy, (d) Ti6Al4V alloy, and (e) Ti5Al2.5Fe alloy

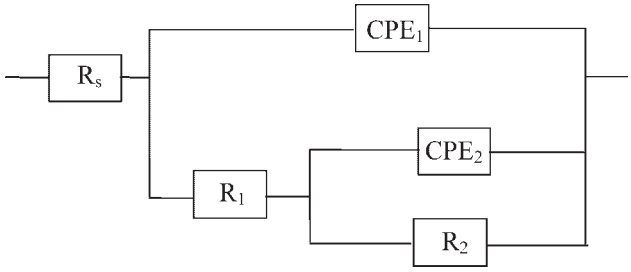

Fig. 8. EC used in the generation of simulated data

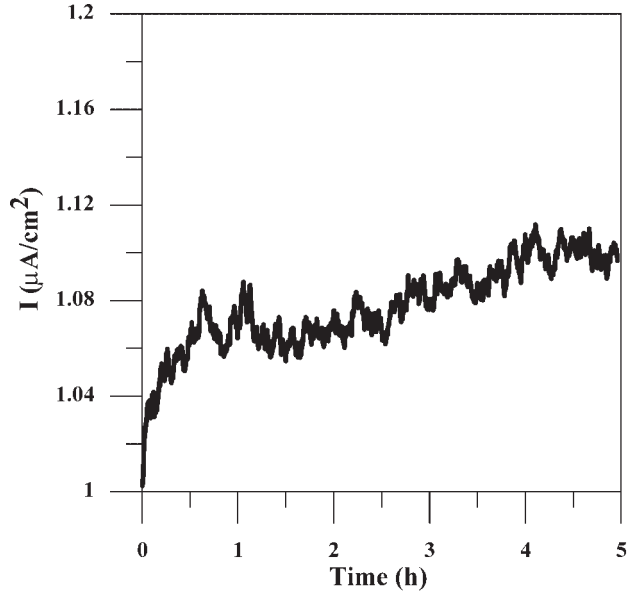

Fig. 9. Plots of I *versus* time for Ti6Al7Nb alloy potentiostatically polarized in artificial saliva at 400 mV/SCE

of alloys. The transpassivation potential is the potential at which the anodic current strongly increases. The potential range situated between the zero corrosion potential (E_{corr}) and the transpssivation potential or pitting potential represents the immunity zone in which corrosion is weak or even insignificant. The more this zone is extended, the less is the risk for the alloy to be in a situation where it can be corroded rapidly by polarization or by galvanic effects (resulted in the presence of another alloy). Table 2 presents the values of the transpasivation potential.

All four alloys and the commercial titanium are characterized by high values of the transpassivation potential (E_{tr}), over 700–800 mV/SCE. From the results of a previous study, it is known that polarization at a potential over 800 mV results in the passive semiconductor layer of TiO_2 being transformed into TiO(OH), which has a higher electronic conductivity [24]:

$$Ti + 3TiO_2 + 2H_2O = 4TiO(OH) \quad (2)$$

For all materials, from 0 to 700 mV/SCE the curves show a passive behavior, and a passive current density in the range 6–17 $\mu A/cm^2$ was estimated. Passive current densities (I_{pass}) are obtained around the middle of the passive range as listed in Table 2. The passive current densities of the samples investigated were of the same order of magnitude. It is well known that if the metal shows lower I_{pass} with longer potential range, the metal is considered to possess a better and more stable passivity. At potentials around 700–800 mV the current density increases due to the transpasivation process.

The corrosion resistance can be estimated by means of the impedance method, also known as EIS, this method being powerful in investigating electrochemical and corrosion systems. This is essentially a steady state technique that is capable of accessing relaxation phenomena whose relaxation times vary over orders of magnitude and permits single averaging within a single experiment to obtain high precision levels.

The EIS spectra are shown in Bode plots of the logarithm of impedance magnitude and of the phase angle as a function of the frequency's logarithm. In Fig. 7, the experimental data are shown as individual points, while the theoretical spectra resulting from the fits to a relevant EC model are shown as lines.

The impedance spectra displayed in Fig. 7 exhibit two time constants for all the samples tested. Those can be divided into two distinct frequency regions: the time constant in the high-frequency part, which arises from the uncompensated ohmic resistance due to the electrolytic solution and the impedance characteristics resulting from the penetration of the electrolyte through a porous film, and the low-frequency part accounting for the processes taking place at the substrate/electrolyte interface [25].

The Bode plots exhibit a two-step or a two time constant system, indicating an oxide with two layers, i.e., a porous outer layer and a compact inner layer [12].

For the interpretation of the electrochemical behavior of a system from EIS spectra, an appropriate physical model of the electrochemical reactions occurring on the electrodes is necessary. The electrochemical cell, because it presents impedance to a small sinusoidal excitation, may be represented by an EC. An EC consists of various arrangements of resistances, capacitors, and other circuit elements, and provides the most relevant corrosion parameters applicable to the substrate/electrolyte system. The usual guidelines for the selection of the best-fit EC were as follows:

– a minimum number of circuit elements were to be employed,

Table 3. The main parameters of the EC

Material	R_s (Ω cm^2)	R_1 (Ω cm^2)	n_1	CPE_1 (S s^n cm^{-2})	R_2 (Ω cm^2)	n_2	CPE_2 (S s^n cm^{-2})
Commercial Titanium	53	5.2×10^5	0.88	9.73×10^{-7}	1.6×10^6	0.96	2.6×10^{-7}
Ti6Al7Nb	54	3.5×10^5	0.88	4.88×10^{-7}	1.4×10^6	0.95	3.21×10^{-7}
Ti6Al2Nb1Ta1Mo	55	1.9×10^5	0.88	5.69×10^{-7}	1.3×10^6	0.95	2.77×10^{-7}
Ti6Al4V	59	1.1×10^5	0.85	7.88×10^{-7}	1.3×10^6	0.94	2.19×10^{-7}
Ti5Al2.5Fe	62	2×10^5	0.85	8.6×10^{-7}	1.4×10^6	0.96	1.34×10^{-7}

– the χ^2 error was suitably low ($\chi^2 < 10^{-4}$), and the error associated with each element was up to 5%.

After testing a number of different electrical circuit models in the analysis of the impedance spectra obtained at the open circuit potential, it was found that the whole set of data for all the samples could be satisfactorily fitted with the EC given in Fig. 8. This is based on the consideration of a two-layer model for the surface film.

The EC is similar to that proposed by *Pan* et al. [12] for titanium immersed in saline solution, by *Gonzalez* and *Mirza-Rosca* [14] for titanium alloys in Ringer type solutions, and by *Luiz de Assis* et al. [26] for titanium alloys in Hank's solution.

Instead of pure capacitors, constant phase elements (CPE) were introduced in the fitting procedure to obtain good agreement between the simulated and experimental data. The impedance of CPE is defined as $Z_{CPE} = 1/Q(j\omega)$ where Q is the combination of properties related to both the surfaces and electroactive species independent of frequency; n is related to a slope of the log Z *versus* log Bode–plots; ω is the angular frequency, and j is imaginary number ($j^2 = -1$). Q is an adjustable parameter used in the fitting routine: when the value of n is equal to 1, the CPE acts as a pure capacitor [13].

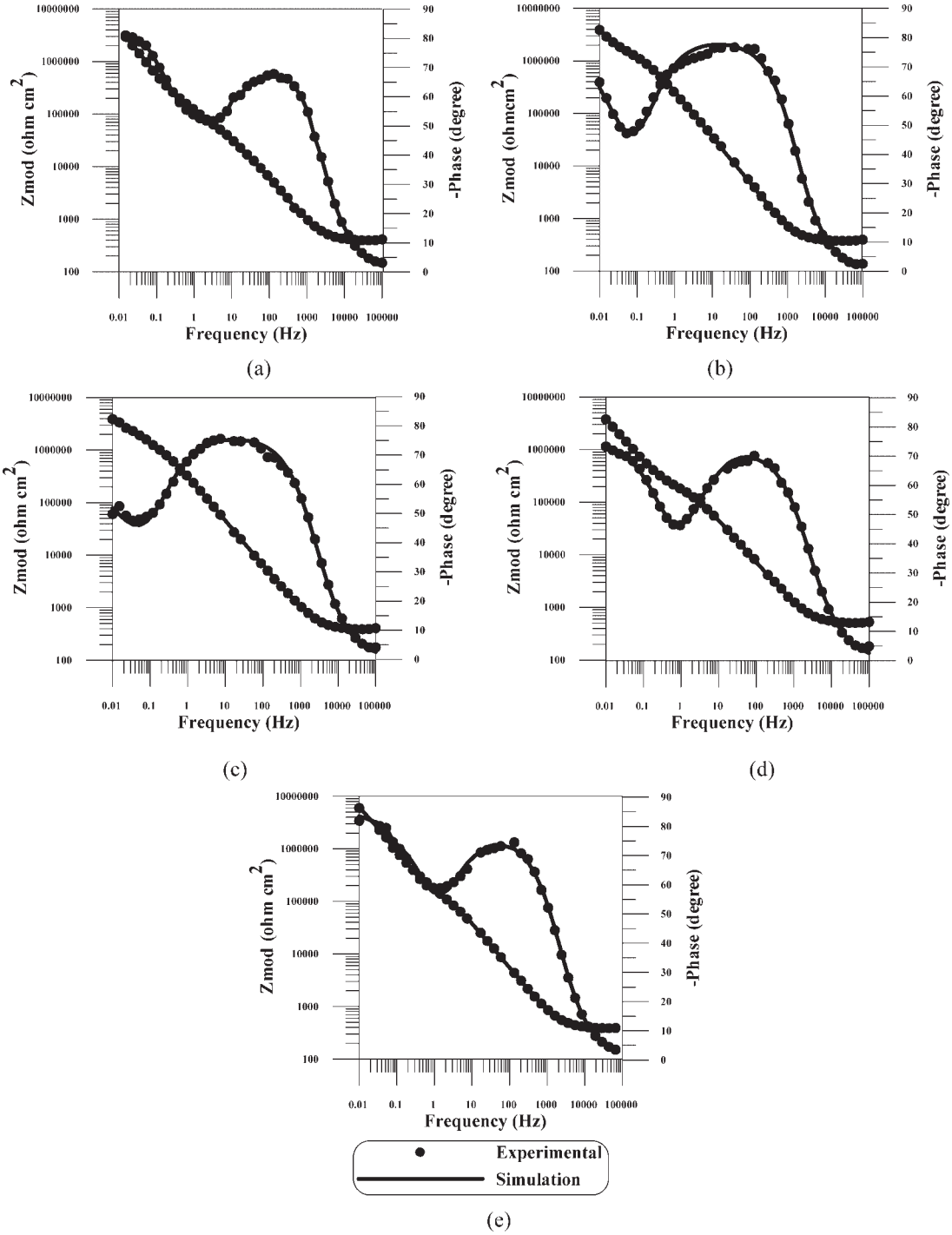

Fig. 10. Bode plots of tested materials recorded at 400 mV/SCE in artificial saliva: (a) Ti6Al2Nb1Ta1Mo alloy, (b) commercial titanium, (c) Ti6Al7Nb alloy, (d) Ti6Al4V alloy, and (e) Ti5Al2.5Fe alloy

Table 4. The main parameters of the EC (for samples polarited at 400 mV/SCE)

Material	R_s (Ω cm^2)	R_1 (Ω cm^2)	n_1	CPE_1 (S s^n cm^{-2})	R_2 (Ω cm^2)	n_2	CPE_2 (S s^n cm^{-2})
Commercial Titanium	65	5.66×10^5	0.88	7.73×10^{-7}	2×10^6	0.96	2.29×10^{-7}
Ti6Al7Nb	54	3.4×10^5	0.85	6.36×10^{-7}	1.7×10^6	0.95	1.59×10^{-7}
Ti6Al2Nb1Ta1Mo	55	1.9×10^5	0.84	7.9×10^{-7}	1.5×10^6	0.95	1.83×10^{-7}
Ti6Al4V	59	2.59×10^5	0.83	6.7×10^{-7}	1.6×10^6	0.95	1.96×10^{-7}
Ti5Al2.5Fe	62	2.02×10^5	0.85	7.6×10^{-7}	1.7×10^6	0.96	1.85×10^{-7}

The components of the EC are:

R_s, ohmic resistance of the electrolyte;
R_1, resistance of the outer porous layer;
R_2, resistance of the compact inner layer;
CPE_1, constant phase element of the outer porous layer;
CPE_2, constant phase element of the compact inner layer.

In Table 3 the main parameters of the proposed EC obtained for all the studied samples are presented.

Polarization resistance (R_p) is represented by the sum of the resistance of the porous oxide layer and the compact oxide layer ($R_1 + R_2$).

The EIS results exhibited capacitive behavior (high corrosion resistance) with phase angle close to -90° and high impedance values (in the order of $10^6\ \Omega\ cm^2$) at medium and low frequencies, which are indicative of the formation of a highly stable film on these materials in the artificial saliva. According to the proposed model, the passive film consists of two layers, the compact inner layer, whose resistance values, R_2, are significantly larger than the values associated to the outer porous layer, R_1, as Table 3 shows. These results indicate that the protection provided by the passive layer is predominantly due to the compact inner layer. Thus, it was found that the commercial titanium has the greatest value of resistance of the compact inner layer.

The value of the fit exponent ''n'' corresponds to the extent of dispersion and is attributed to surface inhomogeneity. The values of the exponent n_2 are approximately 1; then CPE_2 can be said to behave similarly to a pure capacitor. The values of the exponent n_1 are lower than those of n_2; this may be due to higher defectiveness, heterogeneity, and roughness of the outer layer [27].

It is known that pure titanium in the human body may be exposed to potentials of up to 400–500 mV/SCE [28]. The samples were then subjected to chronoamperometry at a constant potential of 400 mV/SCE for 5 h in artificial saliva. Figure 9 shows the current evolution against time for Ti6Al7Nb in artificial saliva, at 400 mV/SCE.

The polarization current of all the specimens at 400 mV/SCE in artificial saliva oscillated around 1 $\mu A/cm^2$. No degradation was observed after the potentiostatic measurements of about 5 h.

Figure 10 shows impedance spectra of titanium materials polarized in artificial saliva at 400 mV/SCE.

Similar plots were obtained for materials polarized in artificial saliva at 400 mV/SCE. No significant change in the shape of the spectra was observed in this case. Among that the rise of the R_2 resistance is small and remains at approximately the same value of $1–2 \times 10^6\ \Omega\ cm^2$.

At 400 mV/SCE, an EC with two time constants was fitted for all samples and is similar to the EC presented in Fig. 8.

In Table 4 the main parameters of the proposed EC obtained for all the studied materials are presented.

Thus, from the data presented in Table 4 it was found that the potential movement to more anodic values (+400 mV/SCE), which can be reached in human body, does not modify the corrosion resistance but even determine a slight increase of that comparatively with the one determined at E_{OC} after a 7 days immersion of samples in artificial saliva.

5 Conclusions

The electrochemical and corrosion behavior of commercial titanium, Ti6Al4V, Ti5Al2.5Fe, Ti6Al7Nb, and Ti6Al2Nb1Ta1Mo was investigated in artificial saliva. All the materials exhibited stable passive polarization behavior; transpassivation potential values (E_{tr}) being higher than 700 mV. Very low corrosion current densities were obtained for all the samples tested in artificial saliva showing that they are passive in this electrolyte. The passivation behavior of Ti5Al2.5Fe, Ti6Al7Nb, and Ti6Al2Nb1Ta1Mo was comparable with that for Ti6Al4V. The EIS Bode plots show two maxima of titanium materials immersed for 7 days in artificial saliva. The EIS spectra results indicated that the film formed on the titanium materials is composed of a bi-layered oxide consisting of an inner barrier layer associated to high impedance and responsible for corrosion protection and an outer porous layer, which apparently facilitates the osseointegration. No significant change in the shape of the spectra was observed in the case of titanium materials polarized in artificial saliva at 400 mV/SCE. The electrochemical and corrosion behavior of Ti6Al4V is not affected on substituting vanadium with niobium, iron, molybdenum, and tantalum.

Acknowledgements: The authors would gratefully acknowledge the financial support of this research by the Ministerio de Ciencia y Tecnologia de Espana under contract DPI 2003-08986.

6 References

[1] R. W. Schutz, D. E. Thomas, *Corrosion of titanium and titanium alloys. Metals Handbook*, Metals Park, Ohio **1978**, 669.
[2] G. H. Hille, *J. Materials* **1966**, *1*, 373.
[3] B. Wälivaara, B. O. Aronsson, M. Rodahl, J. Lausmaa, P. Tengavall, *Biomaterials* **1994**, *15*, 827.
[4] W. F. Ho, C. P. Ju, J. H. Chern Lin, *Biomaterials* **1999**, *20*, 2115.
[5] F. Dabosi, G. Beranger, B. Barow, *Corrosion Localisee*, Les Editions de Physique, Paris **1994**, 637.
[6] M. Pourbaix, *Biomaterials* **1984**, *5*, 122.
[7] M. Meticos-Hucovic, E. Tkalec, A. Kwokal, J. Piljac, *Surf. Coat. Technol.* **2005**, *16*, 540.
[8] F. Contu, B. Elsener, H. Bohni, *J. Biomed. Mater Res.* **2002**, *62*, 412.
[9] M. Aziz-Kerrzo, K. G. Conroy, A. F. Fenelon, S. T. Farrell, C. B. Breslin, *Biomaterials* **2001**, *22*, 1531.

[10] A. Hodgson, Y. Mueller, D. Forster, S. Virtanen, *Electrochim. Acta* **2002**, *41*, 1913.
[11] C. Fonseca, M. A. Barbosa, *Corros. Sci.* **2001**, *43*, 547.
[12] J. Pan, D. Thierry, C. Leygraf, *Electrochim. Acta* 1996, *41*, 1143.
[13] J. Pan, C. Leygraf, D. Thierry, A. M. Ektessabi, *J. Biomed. Mater. Res.* **1997**, *35*, 309.
[14] J. E. G. Gonzalez, J. C. Mirza-Rosca, *J. Electroanal. Chem.* **1999**, *471*, 109.
[15] I. C. Lavos-Valereto, S. Wolynec, I. Ramires, A. C. Guastaldi, I. Costa, *J. Mater. Sci. Mater. Med.* **2004**, *15*, 55.
[16] M. V. Popa, I. Demetrescu, E. Vasilescu, P. Drob, A. S. Lopez, J. C. Mirza-Rosca, C. Vasilescu, D. Ionita, *Electrochem. Acta* **2004**, *49*, 2113.
[17] F. Contu, B. Elsener, H. Bohni, *Corros. Sci.* **2004**, *46*, 2241.
[18] P. Kovacs, *Proceeding of Corrosion 92,* NACE Annual Conference*,* Paper 214, NACE, Houston **1992**.
[19] B. Grosgogeat, L. Reclaru, M. Lissac, F. Dalard, *Biomaterials* **1999**, *20*, 933.
[20] M. Stern, A. Geary, *J. Electrochem. Soc.* **1957**, *104*, 56.
[21] L. Thair, U. Kamachi Mudali, R. Asokamani, B. Raj, *Mater. Corros.* **2004**, *55*, 358.
[22] F. Mansfeld, *J. Electrochem. Soc.* **1973**, *120*, 515.
[23] D. Jones, *Principles and Prevention of Corrosion*, 2nd Edition, Prentice-Hall, Inc., NJ **1996***,* 143.
[24] J. Pjescic, S. Mentus, V. Komnenic, N. Blagojevic, *J. Corros. Sci. Eng.* **2000**, *3*, 7.
[25] R. M. Souto, M. M. Laz, R. L. Reis, *Biomaterials* **2003**, *24*, 4213.
[26] S. Luiz de Assis, S. Wolynec, I. Costa, *Electrochem. Acta* **2006**, *51*, 1815.
[27] R. M. Souto, M. Alanjali, *Corros. Sci.* **2000**, *42*, 2201.
[28] G. Rondelli, B. Vicentini, *Biomaterials* **2002**, *23*, 639.

(Received: January 22, 2007) W 4065
(Accepted: March 5, 2007)